Background Study on Supernova Relic Neutrinos Search in SuperK-Gd

Yang Zhang

Institute of High Energy Physics, Chinese Academy of Sciences, Beijing 100049, China

The Collaborative Innovation Center for Particles and Interactions, Ministry of Education of China

Center for Excellence in Particle Physics, Chinese Academy of Sciences

(Dated: November 1, 2016)

arXiv:1610.09457v1 [hep-ex] 29 Oct 2016

Abstract

The detection of supernova relic neutrinos could provide precious information on the evolution of the universe, the formation of stars, the mechanism of supernova bursts and the related neutrino physics. Many experiments, such as Kamland, Borexino, Sudbury Neutrino Observatory and Super-Kamiokande have conducted searches for the supernova relic neutrinos. However, no supernova relic neutrino signal has been observed until now. This paper reports the background study on the supernova relic neutrinos search for the future neutrino experiment in SuperK-Gd project. The expected event rate for various background sources and supernova relic neutrino models are calculated, respectively.

PACS numbers: 13.15.+g, 13.85.Rm, 97.60.Bw, 29.90.+r

I. INTRODUCTION

Supernova relic neutrinos (SRN), also known as diffuse supernova neutrino background (DSNB), are six types of neutrinos from all the past core-collapse supernovae since the beginning of the universe. The differential flux of SRN on earth can be calculated using the supernova rate, neutrino emission spectrum from a supernova and the redshift [1, 2]. The detection of supernova relic neutrinos could provide precious information on the evolution of the universe, the formation of stars, the mechanism of supernova bursts and the related neutrino physics. In hydrogen-riched targets such as scintillator and water Cherenkov detectors, SRN are most likely to be detected by inverse-beta-decay (IBD) reaction ($\bar{\nu}_e + p \rightarrow e^+ + n$). Therefore, we focus on the SRN $\bar{\nu}_e$ only in this article. Many theoretical models like constant supernova rate model (referred to as const SN) [3], population synthesis model [4], cosmic gas infall model [5], chemical evolution model [6], heavy metal model [7, 8], large mixing angle (LMA) model [9], star formation model [10], failed supernova model [11], HBD 6 MeV model [12], have constructed the flux and spectrum of SRN based on the assumption of different supernova rate and neutrino emission spectrum. Due to a tiny cross section of neutrino interaction [13], the detection of SRN needs a huge target mass. The SRN have not been observed until now and the current best flux upper limits are given by Super-Kamiokande (SK) [14, 15] and Kamland [16] experiments. These limits are approaching theoretical predictions.

SK is the world largest water Cherenkov detector, which has 50,000 tons pure water as the target mass. The huge mass makes SK a ideal position to make the detection of SRN possible. Due to the large radioactive background from the surrounding wall, PMTs and their housings, events within two meters to the inner detector wall are removed. This results in a fiducial volume (FV) of 22.5 kton for the detector. Using the cross section of IBD reaction in Ref. [13], the expected SRN $\bar{\nu}_e$ events rate at SK with different theoretical models mentioned above are shown in Fig. 1.

Perhaps the best energy window for the SRN search is 11.3-31.3 MeV (referred to as "golden" energy window). The reactor neutrinos have a typical energy up to about 10 MeV, however, the resolution effect at SK could extend the energy to higher region by 1-2 MeV. While above 31.3 MeV, the atmospheric neutrinos $\bar{\nu}_e$'s which have the same signature as the SRN $\bar{\nu}_e$ are dominant [18]. In the "golden" energy window, the major backgrounds

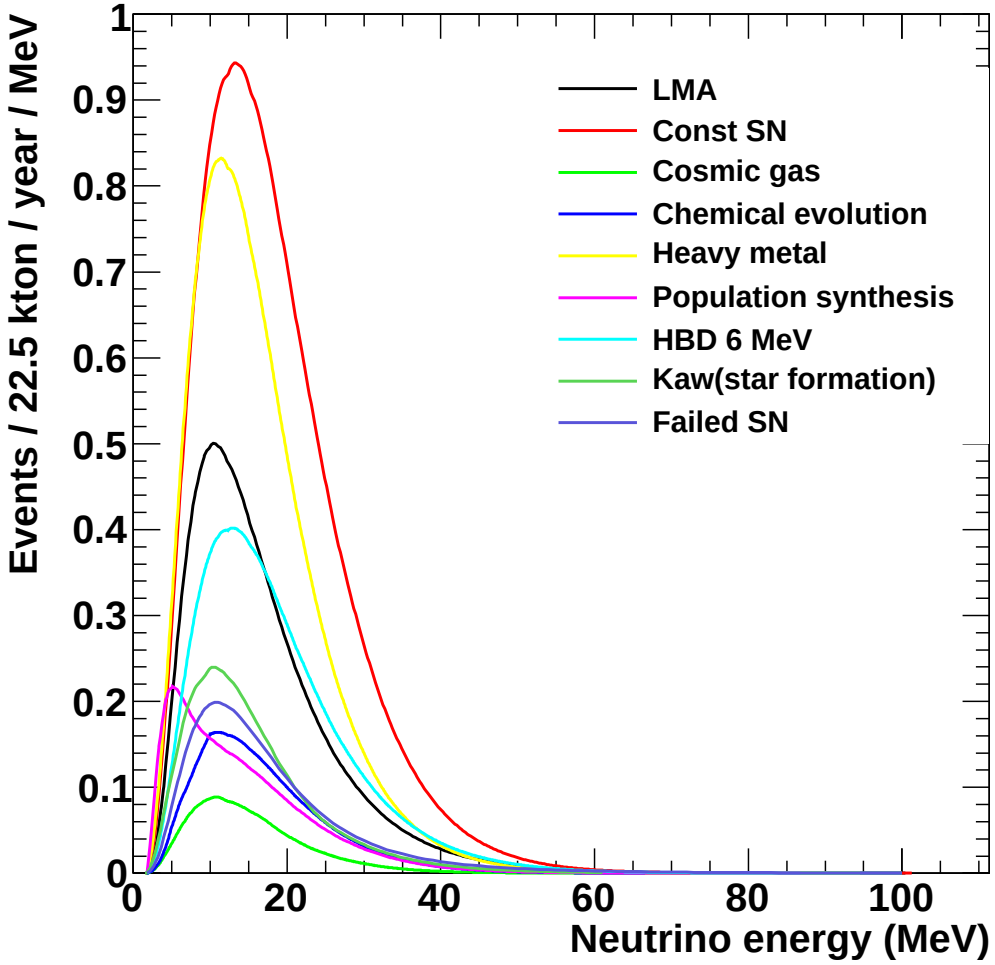


Fig. 1: The expected events rate of SRN $\bar{\nu}_e$ at SK using different theoretical models.

for SRN search are the radioactive isotopes induced by cosmic-ray muons spallation [17], invisible muon events and irreducible atmospheric neutrino $\bar{\nu}_e$. Most of the decay products from radioactive isotopes are β or $\beta\gamma$ only without an accompanied neutron, and thus they can be removed by the identification of delayed neutron detection. Ref. [15] performed a search for SRN in 13.3-31.1 MeV by tagging delayed neutron, whose capture on hydrogen ($n + p \rightarrow d + \gamma$) can emit a 2.2 MeV γ. The efficiency of neutron tagging is ~20% with a corresponding background probability of ~1% for uncorrelated events (dark noise and low-energy radioactivity) mis-tagged as a neutron in a time length of 500 μs. Using this technique, the spallation backgrounds without the neutron in the decay are greatly reduced by about two order of magnitude. The lower edge of the SRN search energy window is

lowered by 4 MeV from 17.3 MeV compared to the previous search [14] without the neutron tagging. However, the spallation background are still overwhelming below 15.3 MeV of neutrino energy due to the low photon yield of the 2.2 MeV γ. To increase the signal-to-noise ratio, Ref. [18] has proposed to add 0.2% gadolinium into SK water. The neutron capture on gadolinium could emit an 8 MeV γ cascade, and thus the neutrons can be easily detected with high efficiency. This proposal is formally approved by the SK collaboration in the summer of 2015 after comprehensive studies and is referred to as SuperK-Gd project [17]. In this article, the detailed study of the expected events rate for various background sources and SRN models at SuperK-Gd project is presented.

II. BACKGROUND SOURCES

A. Accidental background

Two uncorrelated events of a single electron and an event (uncorrelated neutron and non-neutron event) reconstructed as a neutron could coincide to pass the identification of IBD events. Since SK cannot differentiate between the electron and positron, we use electron to represent both the electron and positron. Ref. [19] demonstrated for the time that the 8 MeV γ cascade from Gd was observable in water. The total energy of the detected γ's peaks around 4.3 MeV due to the Cherenkov threshold of the Compton scattered electons. The neutron tagging is optimal when a 3 MeV cut the for delayed neutron is set. At this point, the neutron tagging efficiency is 66.7% with the corresponding background probability of 2×10^{-4}. In practice, the efficiency of neutron tagging would be much higher since the experiment was performed in a small calibration source. In this article, the efficiency of 80% (90% for capture and 90% for reconstruction) for neutron tagging on Gd is assumed. From solar neutrinos study [20], we know that the single electrons rate below 6 MeV are dominated by the radioactive impurities of the inner detector itself, while above 6 MeV the spallation background induced by the cosmic ray muons are dominated. The golden energy window does not overlap with that of the internal radioactive impurities, and this background is negligible in the SRN search study. About 95% of the radioactive isotopes induced by cosmic-ray muon spallation are removed by the spallation cut at SK. The spallation cut is performed with a likelihood function based on the information of time and distance of the

low-energy events to the preceding muons as well as the energy deposition (dE/dx) of muon along its track. The lifetimes of the isotopes vary from 0.01 to 19.9 s. Due to a muon rate of $\sim$2 Hz, isotopes with longer lifetimes could survive the spallation cut. The remaining number of the spallation background events in the golden energy window is estimated to be 2.9×10^3 /22.5 kton/year [19] after the spallation cut. Consequently, the remaining spallation background without neutron in the decay after neutron tagging is calculated to be about 0.6 events/22.5 kton/year by taking the background probability into account. The events rate of solar neutrinos (ν_e only) at SK is about 10 events/22.5 kton/day, however, the scattered electrons ($\nu_e + e^- \to \nu_e + e^-$) retain the direction of the incident solar neutrinos. Hence, more than 95% of them can be removed by this direction (so called solar angle) cut. This cut can even be loosed due to the strong background suppression of neutron tagging. Finally, the remaining solar neutrino events can be negligible.

B. ^{8}He/^{9}Li background

The cascade decays of radioactive isotopes with a β and a neutron can mimic the IBD reaction, and thus can be a dangerous background for the SRN search. Ref. [17] measured the yield for each major radioactive isotope induced by cosmic-ray muon spallation at SK for the first time. This is quite useful in estimating the contamination of the spallation background to the SRN search since the individual contribution can be evaluated in a case-by-case basis. Both ^{8}He and ^{9}Li can have the βn decay modes. From the SK measurement, the production rate of ^{8}He was consistent with zero and only upper limit was given. In addition, the endpoint energy of ^{8}He for the βn decay mode is below the lower edge of the "golden" energy window even if the energy resolution is considered. As a result, we found only ^{9}Li can have a significant contribution to the SRN search in the "golden" energy window through the β energy tail. From the theoretical point of view, ^{9}Li is mainly produced by the secondary π^- scattering on the oxygen nucleus [21]. The measured production rate of ^{9}Li at SK is $0.86 \pm 0.12 \pm 0.16$ /kton/day, which leads to about 3,600 ^{9}Li βn events/22.5 kton/year by taking into account the branching ratio of $(50.8 \pm 0.9)\%$ for the βn decay mode [22]. With the present spallation cut at SK, we assume a 0.5% leakage of ^{9}Li background and 80% efficiency for the SRN signal. Fig. 2 shows the expected spectrum for ^{9}Li background and SRN signal using the LMA model. The β spectrum for ^{9}Li βn decay mode is obtained

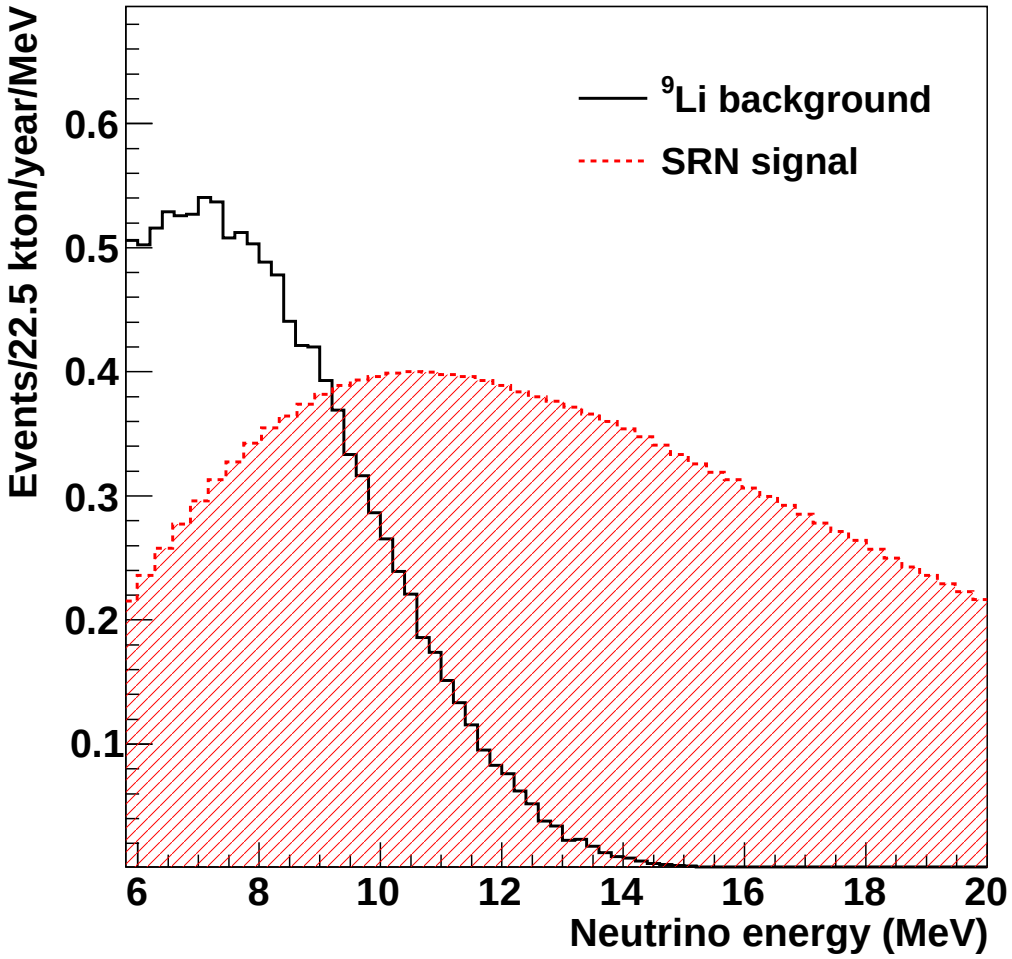


Fig. 2: The expected spectrum for ^{9}Li background (solid) and SRN signal (hatched) using the LMA model [9], assuming 80% signal efficiency.

from Ref [23] by taking into account the resolution effect of SK. The number of ^{9}Li $\beta + n$ events is estimated to be $0.5 \pm 0.1 \pm 0.2$ /22.5 kton/year above 11.3 MeV of the neutrino energy ($E_{\bar{\nu}_e} \simeq E_{e^+} + 1.3$ MeV), in which more than half of them distribute between 11.3-12.3 MeV of the neutrino energy. By increasing the lower edge of the SRN search energy window, the ^{9}Li background could be further removed greatly while the SRN signal reduces slightly due to its more flatter spectrum. The increase will also help remove the occasional upward fluctuated reactor antineutrinos described in section 2.3.

C. Geo- and reactor neutrinos

The energy of geo-neutrinos from uranium, thorium and potassium in the earth is low (up to 4.5 MeV for ^{238}U, 2.3 MeV for ^{232}Th and 1.3 MeV for ^{40}K). Hence, the contribution from geo-neutrinos vanishes. The reactor antineutrinos have an energy up to ∼10 MeV [24, 25], however, they could extend to higher energy due to the SK energy resolution. Most of the nuclear power plants (NPP) in Japan were shut down after the Fukushima accident in 2011, and the reactor neutrino background could be negligible in this case. In the worst case that the all the NPP in Japan are reopened, the expected events rate of reactor antineutrino in the "golden" energy window for the SRN search can be estimated from the Kamland results [16], which is 2.2 events above 8.3 MeV of neutrino energy for an exposure of 4.53 kton·year. By scaling the value to SK one-year exposure and taking the spectrum of the reactor neutrinos into account (the fraction of reactor antineutrinos is about 1% above 11.3 MeV over that above 8.3 MeV), we estimated the number of reactor antineutrino leakage to be 0.1 events/22.5 kton/year.

D. Atmospheric neutrinos

Atmospheric $\nu_\mu/\bar{\nu}_\mu$ can interact with the nucleons via the charge current processes and produce muons. Sometimes these muons are below the Cherenkov threshold and are called invisible muons. The electrons from these invisible muon decays follow a Michel spectrum and cannot be tagged as background individually. Atmospheric $\bar{\nu}_e$ have exactly the same signature as the SRN $\bar{\nu}_e$ and can only be differentiated from the spectrum, while atmospheric ν_e only have the single electrons in the final states. Fig.2 in Ref. [26] and Fig.11 in Ref. [14] show the spectra of the remaining backgrounds induced by atmospheric neutrinos for the SRN search above 19.3 MeV and 17.3 MeV of neutrino energy, respectively. The high end of energy window for these two searches were both around 90 MeV. In these searches, only a prompt electron was required since no neutron tagging was performed. The major background in these two analyses were from atmospheric $\nu_\mu/\bar{\nu}_\mu$ and $\nu_e/\bar{\nu}_e$ and can be greatly reduced when the high end of the energy window is lowered. Fig.3 in Ref. [15] shows the spectrum for the SRN search with neutron tagging in the energy range of 13.3-31.3 MeV. In this figure, the data points below 18 MeV are mainly from the remaining spallation

TABLE I: The expected number of background events together with the SRN signal events in the "golden" energy window. The unit is events /22.5 kton/year.

Accidental	^{9}Li	Reactor $\bar{\nu}_e$	Atmospheric $\bar{\nu}_\mu$	Atmospheric $\bar{\nu}_e$	SRN models
0.6	0.5	0.1	7	1	1-13

background and that above are mainly from atmospheric $\bar{\nu}_\mu$ induced invisible muon events. There is a possibility of neutral current background events, which are induced by the reaction of $\nu + {}^{16}O \rightarrow \nu + {}^{15}O^\star + n$; ${}^{15}O^\star \rightarrow {}^{15}O + \gamma$ ($\sim$6 MeV); the produced neutron could further collide with the nucleus and secondary γ's could be emitted. Sometimes the total reconstructed energy of these γ's could be located in the interested energy range. However, no evidence of neutral current events is observed [15]. Hence, we ignore this category of background in this article. The number of expected invisible muon events is estimated to be about 15 events/22.5 kton/year in the "golden" energy window from Ref. [26]. With the neutron tagging, the contribution from atmospheric ν_μ could be negligible. As a result, we assume the number of invisible muon events to be 7 events/22.5 kton/year due to the similar fluxes of atmospheric ν_μ and $\bar{\nu}_\mu$ [27] and the same order for cross sections of $\bar{\nu}_\mu + p \rightarrow \mu^+ + n$ and $\nu_\mu + n \rightarrow \mu^- + p$. This evaluated number is consistent with the value by scaling the four events above 16 MeV in Fig.3 of Ref. [15] taking into the live time of 960 days and neutron tagging efficiency of 20% into account. The number of atmospheric $\bar{\nu}_e$ is relatively small, and we estimate the number to be about 1 events/22.5 kton/year in the interested energy range by considering the flux and IBD cross section as well as the neutrino oscillation.

III. SRN SIGNAL

The expected number of SRN signal events for various theoretical models (shown in Fig. 1) is within the range of 1-13 events /22.5 kton/year in the "golden" energy window. The numbers of background and SRN signal events are summarized in Table I. Although the const SN model was already excluded by the SK-I results [26], further results from SK [14, 15] have no strong constraint on this model. We still use this value for one of the predictions.

IV. SUMMARY AND OUTLOOKS

A detailed study of various background sources for the search of SRN in SuperK-Gd project is presented here. The estimations of the background events are relatively reliable since they are based on the existing data. In the SuperK-Gd project, the signal-to-noise ratio would be unprecedentedly high although the search is still background limited. The dominate background are the invisible muons induced by the atmospheric neutrinos. Discovery of SRN using one-year data taking is probably not reasonable based on the present theoretical frames. However, long-term (e.g. 5-year) data taking would make the detection of SRN possible since its spectrum differs from all the background.

[1] J. F. Beacom, Ann. Rev. Nucl. Part. Sci. 60 (2010) 439

[2] S. Ando and K. Sato, New J. Phys. 6 (2004) 170

[3] T. Totani and K. Sato, Astropart. Phys. 3, 367 (1995).

[4] T. Totani, K. Sato and Y. Yoshii, Astrophys. J. 460, 303 (1996).

[5] R. A. Malaney, Astropart. Phys. 7, 125 (1997).

[6] D. H. Hartmann and S. E. Woosley, Astropart. Phys. 7, 137 (1997).

[7] M. Kaplinghat, G. Steigman and T. P. Walker, Phys. Rev. D 62, 043001 (2000).

[8] L. Strigari, M. Kaplinghat, G. Steigman and T. Walker, JCAP, 0403:007 (2004).

[9] S. Ando, K. Sato and T. Totani, Astropart. Phys. 18, 307 (2003).

[10] M. Fukugita and M.Kawasaki, Mon. Not. Roy. Astron. Soc. 340, L7 (2003).

[11] C. Lunardini, Phys. Rev. Lett. 102, 231101(2009).

[12] S. Horiuchi, J. F. Beacom and E. Dwek, Phys. Rev. D 79, 083013 (2009).

[13] A. Strumia and F. Vissani, Phys. Lett. B 564 (2003) 42

[14] K. Bays *et al.*, (Super-Kamiokande Collaboration), Phys. Rev. D 85, 052007 (2012).

[15] H. Zhang *et al.*, (Super-Kamiokande Collaboration), Astropart. Phys. 60 (2015) 41.

[16] A. Gando, *et al.*, (KamLAND Collaboration), Astrophys. J., 745 (2012), 193

[17] Y. Zhang *et al.*, (Super-Kamiokande Collaboration), Phys. Rev. D 93, 012004 (2016)

[18] J. F. Beacom and M. R. Vagins, Phys. Rev. Lett., 2004, **93**: 171101.

[19] H. Watanabe *et al.*, (Super-Kamiokande Collaboration), Astropart. Phys., 2009, **31**: 320.

[20] K. Abe *et al.*, (The Super-Kamiokande Collaboration), Phys. Rev. D 83, 052010 (2011)

[21] S. W. Li, J. F. Beacom, Phys. Rev. C 89, 045801 (2014).

[22] D. R. Tilley, J. H. Kelley, J. L. Godwin, D. J. Millener, J. E. Purcell, C. G. Sheu, and H. R. Weller, Nucl. Phys. A 745, 155 (2004).

[23] http://www.tunl.duke.edu/nucldata/GroundStatedecays/

[24] A. Gando *et al.*, (KamLAND Collaboration) Phys. Rev. D 88, 033001 (2013).

[25] F.P. An *et al.*, (Daya Bay Collaboration), Phys. Rev. D 90, 071101 (2014).

[26] M. Malek *et al.* (Super-Kamiokande Collaboration) Phys. Rev. Lett. 90, 061101 (2003)

[27] M. Honda, T. Kajita, K. Kasahara, S. Midorikawa, and T. Sanuki, Phys. Rev. D 75, (2007) 043006